Aluminum/Sulfur Batteries Hot Paper

Deutsche Ausgabe: DOI: 10.1002/ange.201603531
Internationale Ausgabe: DOI: 10.1002/anie.201603531

A Rechargeable Al/S Battery with an Ionic-Liquid Electrolyte

Tao Gao, Xiaogang Li, Xiwen Wang, Junkai Hu, Fudong Han, Xiulin Fan, Liumin Suo, Alex J Pearse, Sang Bok Lee, Gary W. Rubloff, Karen J Gaskell, Malachi Noked, and Chunsheng Wang**

Abstract: *Aluminum metal is a promising anode material for next generation rechargeable batteries owing to its abundance, potentially dendrite-free deposition, and high capacity. The rechargeable aluminum/sulfur (Al/S) battery is of great interest owing to its high energy density (1340 Wh kg^{-1}) and low cost. However, Al/S chemistry suffers poor reversibility owing to the difficulty of oxidizing AlS_x. Herein, we demonstrate the first reversible Al/S battery in ionic-liquid electrolyte with an activated carbon cloth/sulfur composite cathode. Electrochemical, spectroscopic, and microscopic results suggest that sulfur undergoes a solid-state conversion reaction in the electrolyte. Kinetics analysis identifies that the slow solid-state sulfur conversion reaction causes large voltage hysteresis and limits the energy efficiency of the system.*

Rechargeable aluminum batteries (RABs) based on Al metal anodes have attracted lots of attention recently as one promising beyond-lithium-ion-battery system because Al provides a very high capacity (2.98 Ah g^{-1} and 8.05 Ah cm^{-3}) and it is the most abundant metal element in the earth's crust. Although reversible Al deposition/stripping in non-aqueous electrolyte at room temperature is challenging owing to the tendency of Al to form a surface passivation layer,[1] it was shown to be possible in ionic liquid-based electrolyte with up to 100% Coulombic efficiency.[2] Generally, previous reports of RABs using ionic-liquid electrolyte can be summarized into two categories according to their distinctive cathode reactions. The first category functions by anion (Cl^-, $Al_xCl_y^-$,etc.) insertion into graphite or other carbonaceous materials.[3–6] This dual-ion operation mechanism inevitably induces electrolyte concentration decline during battery charging. Consequently, the attainable energy density of the battery is compromised by the amount of salt in the electrolyte. The other category is a rocking-chair system which functions by Al^{3+} intercalation at cathode. This type is more preferred since the overall electrolyte concentration remains constant during battery operation. Nevertheless, previous investigations show inferior performance.[7,8] To realize the promising metrics of RAB, there is a need for developing high voltage/capacity cathodes.

As a high capacity cathode material (1675 mAh g^{-1}), sulfur has attracted intense interest in Li/S,[9,10] Mg/S,[11,12] and Na/S[13,14] systems. A rechargeable Al/S battery is also of great interest because of its high cell capacity (1072 mAh g^{-1} of total electrode mass), reasonable voltage (1.25 V), and low cost. Overall, the gravimetric energy density is 1340 Wh kg^{-1}, over three-times that of a commercial $LiCoO_2$/graphite cell and close to that of a Li_2S/silicon cell.[12] The high energy density and low cost makes the Al/S system a very promising battery system for electric vehicles and grid energy storage. Motivated by this potential, Cohn et al. recently demonstrated a primary Al/S battery with capacity close to the theoretical value.[15] Up to now, there was no demonstration of reversible Al/S battery owing to the inability to oxidize AlS_x. Herein, we demonstrate the first reversible Al/S battery in an ionic-liquid electrolyte by enhancing the oxidation kinetics of AlS_x via encapsulating sulfur into microporous activated carbon (pore size <2 nm). Electrochemical, spectroscopic, and microscopic observations indicate that sulfur undergoes a solid-state conversion reaction. Kinetics analysis suggests that the system is limited by this slow solid-state sulfur conversion reaction. Raising temperature was shown to be an effective approach to overcome the kinetic limitation and thus decrease the voltage hysteresis.

The room temperature ionic-liquid electrolyte was made by mixing $AlCl_3$ with 1-ethyl-3-methylimidazolium chloride (EMIC) in an atomic ratio of 1.3:1. The activated carbon cloth (ACC)/sulfur composite was fabricated following previous reports.[10,16] N_2 adsorption/desorption isotherm shows type I behavior (Figure S1 in the Supporting Information), indicating the microporous structure of ACC. The Brunnauer–Emmett–Teller (BET) specific surface area decreases significantly from 2376.6 m^2 g^{-1} to 1532.8 m^2 g^{-1} and the micropore volume decreases from 0.93 cm^3 g^{-1} to 0.61 cm^3 g^{-1} after sulfur impregnation. A typical charge/discharge curve of the ACC/S cathode in Li/S battery is given in Figure S2. Aluminum deposition/striping and the anodic stability of the electrolyte on glassy carbon are given in Figure 1 a. The deposition of Al occurs through the reduction of $Al_2Cl_7^-$ to Al,[2] which starts at a low over-potential and proceeds at very fast kinetics (-30 mA cm^{-2} at -0.5 V vs. Al reference electrode; Figure 1 a). Charge balance curve (the inset of Figure 1 a) shows the deposition/striping process is highly reversible with

[*] T. Gao, X. Li, X. Wang, F. Han, Dr. X. Fan, Dr. L. Suo, Prof. C. Wang
Department of Chemical and Bimolecular Engineering
University of Maryland
College Park, MD 20740 (USA)
E-mail: cwang@umd.edu
A. J. Pearse, Prof. G. W. Rubloff, Dr. M. Noked
Department of Material Science and Engineering
University of Maryland
College Park, MD 20740 (USA)
E-mail: mnoked@gmail.com
Dr. J. Hu, Prof. S. B. Lee, Dr. K. J. Gaskell, Dr. M. Noked
Department of Chemistry and Biochemistry, University of Maryland
College Park, MD 20740 (USA)

Supporting information for this article can be found under: http://dx.doi.org/10.1002/anie.201603531.

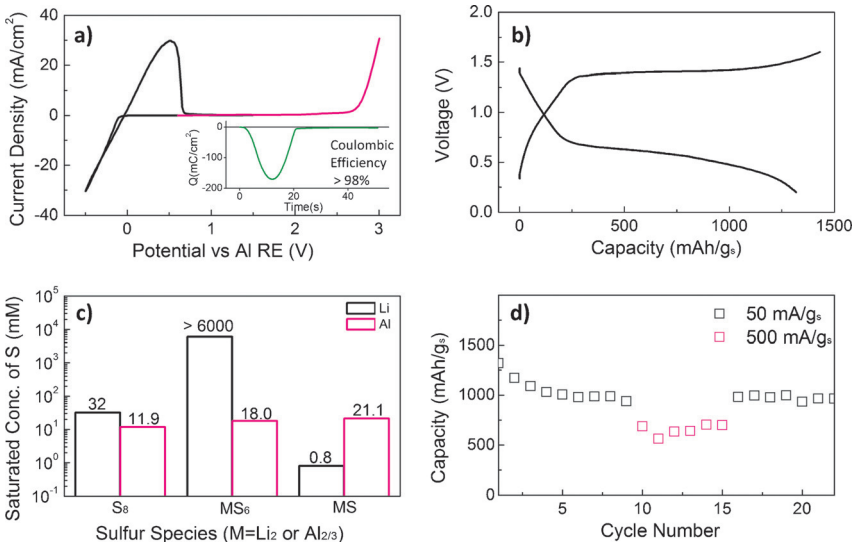

Figure 1. a) Al deposition/striping in EMIC:$AlCl_3$ = 1:1.3 electrolyte (black) and the electrochemical stability of the electrolyte (pink). Inset: Charge–time curve of Al deposition/stripping. Scan rate: 100 mV s^{-1}, working electrode (WE): Glassy carbon; counter electrode (CE) and reference electrode (RE): Al wire. b) A typical charge/discharge curve of the Al/S battery at room temperature with ACC/S cathode, ionic-liquid electrolyte, and Al foil anode. Current: 50 mA g_s^{-1}. c) Solubility of different sulfur species (in units of sulfur atomic concentration) in Li and Al electrolytes. Li electrolyte is 1 M LiTFSI in TEGDME. The solubility of lithium polysulfide is from Ref. [20] and [21]. d) Cycling stability of the Al/S cell.

a Coulombic Efficiency close to 100%. The electrolyte is thermodynamically stable up to around 2.7 V on an inert current collector (glassy carbon) (Figure 1a), where anodic decomposition occurs ($4\,AlCl_4^- \rightarrow 2\,Al_2Cl_7^- + Cl_2 \uparrow + 2e^-$).[2] On a non-inert current collector (Inconel alloy), the electrolyte is also stable up to 2.7 V except for self limited interfacial instability on the Inconel at 1.35 V. At this potential, corrosion of Inconel alloy leads to surface passivation, which ensures kinetic stability (Figure S3–S5). For this reason, Inconel alloy was used as cathode current collector for testing Al/S battery.

The Al/S battery was made by coupling the ACC/S cathode with an Al foil anode in a Swagelok cell. The typical charge/discharge profile of the Al/S cell at 50 mA g_s^{-1} shows a single discharge (ca. 0.65 V) and charge plateau (1.40 V) (Figure 1b). This behavior is quite distinctive from the typical two-stage voltage profile in Li/S system[9,10] (Figure S2) or Mg/S system[11,12] using ether-based electrolyte, but resembles Li/S system based on some ionic liquid electrolyte,[17,18] and solid state Li/S battery,[19] implying a similar reaction mechanism: a solid-state conversion reaction of sulfur to aluminum sulfide. To confirm this hypothesis we first measured the solubility of different sulfur species in the ionic liquid electrolyte. As presented in Figure 1c, sulfur, "aluminum polysulfide" ($Al_{2/3}S_6$) and aluminum sulfide (Al_2S_3) have similar low solubility (very slightly soluble). Their solubility is comparable to that of sulfur in tetraglyme, but is two orders of magnitude lower than Li polysulfide (Li_2S_6; see more explanation of the terms in the Supporting Information).[20,21] Moreover, ICP-OES shows low sulfur loss into the electrolyte after cycling (5.9 ± 1.1 wt% of all loaded sulfur compared to 25 wt% in ether-based Li/S cells).[9] These results support the notion that sulfur undergoes a solid-state conversion reaction. A maximum capacity of approximately 1320 mAh g_s^{-1} can be obtained at 50 mA g_s^{-1}, corresponding to a sulfur utilization of 58% after excluding the contribution of activated carbon (Figure S6). Remarkably, cycling stability demonstrates 1000 mAh g_s^{-1} for over 20 cycles (Figure 1d), illustrating the substantially improved reversibility for the sulfur reduction/oxidation reaction. High loading electrodes (>1 mg cm^{-2}) suffer low sulfur utilization. Still, they show reversible behavior (Figure S7).[15] The enhanced reversibility in our system could be explained by the confinement of the reduced AlS_x species in the micropores (<2 nm), which effectively facilitates sulfide oxidation kinetics upon charging owing to its ready electron access, large reaction area, and shortened solid state Al^{3+} diffusion length. Additionally, the low sulfur loss also benefits the high stability of this system.

Spectroscopic and microscopic measurements were performed to understand the reaction mechanism. X-ray diffraction (XRD) was conducted to examine the phase change of sulfur in the Al/S battery (Figure 2a, for material characterization see Supporting Information). After discharge all the sulfur peaks disappeared as a result of its electrochemical reduction but no new peaks emerge. X-ray photoelectron spectroscopy (XPS) was conducted to examine the oxidation state change of sulfur species. The S 2p and

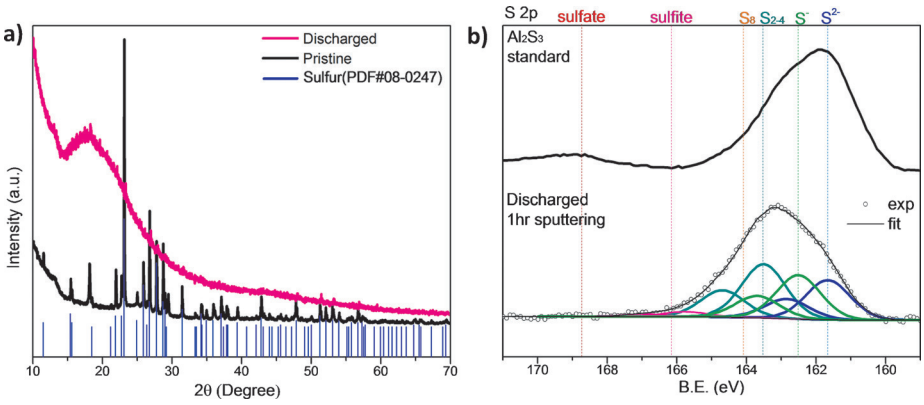

Figure 2. a) XRD pattern of the sulfur cathode before and after discharge. The bump at 15° comes from the sealing tape. b) High resolution S 2p spectra of Al_2S_3 standard and discharged ACC/S with 1 h sputtering.

Al 2p spectrum of Al_2S_3 powder was measured as reference (Figure S8). The XPS depth profile of the discharged ACC/S was collected at different Ar sputtering durations to avoid the influence of surface residual electrolyte following a previous study[22] (Figure S9, see discussion in Supporting Information). The S 2p spectrum of discharged ACC/S with 1 h sputtering is given in Figure 2b with the spectrum of Al_2S_3 plotted for comparison. Fitted with constrained spin-orbit split doublets, the S 2p spectrum of discharged ACC/S consists of four components located at 161.7 ± 0.1 eV, 162.5 ± 0.1 eV, 163.4 ± 0.1 eV, and 165.7 ± 0.1 eV, which are assigned to fully reduced sulfur (S^{2-}), partially reduced sulfur (S^{-}), elemental sulfur (S_{2-4}) and sulfite, respectively. Note that not all the sulfur has been fully reduced, which is in good agreement with the electrochemical results, showing that at room temperature the sulfur utilization in the ACC/S cathode cannot reach 100%. Also note the surface of Al anode is free of dendrite after cycling (Figure S10). Based on these results, the reaction mechanism during discharge/charge was suggested as Scheme 1.

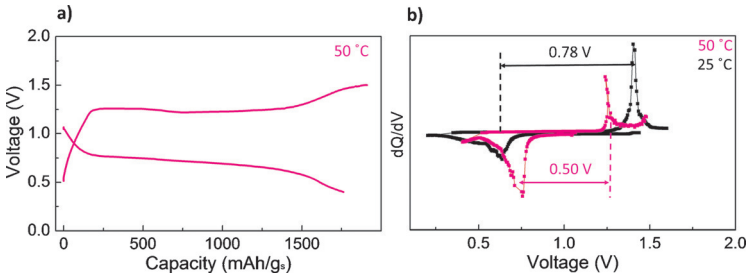

Figure 3. a) Charge/discharge curve at 50 °C (50 mA g_s^{-1}). b) dQ/dV curves of Al/S cell at different temperatures.

$$\text{Anode:}\quad 2Al + 14AlCl_4^- \underset{\text{Charge}}{\overset{\text{Discharge}}{\rightleftharpoons}} 8Al_2Cl_7^- + 6e^-$$

$$\text{Cathode:}\quad 8Al_2Cl_7^- + 6e^- + 3S \underset{\text{Charge}}{\overset{\text{Discharge}}{\rightleftharpoons}} Al_2S_3 + 14AlCl_4^-$$

Scheme 1. Discharge/charge reaction equations for the Al/S battery at anode and cathode.

A large voltage hysteresis (ca. 0.78 V at 50 mA g_s^{-1}) was observed during charge/discharge (Figure 1b, Figure S11), which leads to a low roundtrip efficiency of the Al/S system. Among all kinetics inhibitors, ohmic resistance and anode charge-transfer resistance are negligible owing to the electrolyte's high conductivity (15 mS cm^{-1} at 30 °C)[2] and fast Al deposition/striping kinetics (Figure 1a). Electrochemical impedance spectroscopy (EIS) results confirmed this hypothesis and further pointed out that cathode charge transfer contributes significantly to the overall voltage loss (Figure S12), which is expected for the solid-state sulfur conversion reaction. Additionally, polarization resulting from the sluggish Al^{3+} diffusion in the AlS_x and S/AlS_x phase boundary movement should also have a large impact on the kinetics. A depolarization experiment was performed to evaluate the magnitude of these polarizations (Figure S13): A sudden voltage jump of < 0.15 V, accounting for the fast removal of ohmic overpotential and charge-transfer overpotential, was observed immediately after the applied current was withdrawn. In contrast, it takes more than 24 h to eliminate other polarizations (> 0.3 V) and relax the battery potential to equilibrium. Thus, the Al/S battery is kinetically limited by the solid-state sulfur conversion reaction (including interfacial charge transfer, subsequent Al^{3+} diffusion, and phase-boundary movement). To overcome the polarizations, we intentionally elevated the experiment temperature to 50 °C. The discharge plateau was raised to 0.75 V and the charge plateau was lowered to 1.25 V as a result of the expedited kinetics (Figure 3a). A clear decline in voltage hysteresis to 0.5 V was observed from dQ/dV curve (Figure 3b). A high capacity of 1750 mAh g_s^{-1} (including the capacitive storage of carbon) reveals higher sulfur utilization of 83%.

In conclusion, we demonstrated the first rechargeable Al/S battery with an ionic-liquid electrolyte, by addressing the hurdle for oxidizing AlS_x through confining sulfur species into microporous carbon (pore size < 2 nm), which can improve the electron access of sulfur species, enlarge the interfacial reaction area, and reduce the Al^{3+} diffusion length. Experimental results indicate that sulfur undergoes a solid-state conversion reaction in this system. The readiness to oxidize AlS_x and low sulfur loss into the electrolyte give a substantially improved reversibility: a capacity of 1000 mAh g_s^{-1} for over 20 cycles, corresponding to an obtainable energy density of 650 Wh kg^{-1}. Moreover, the Al/S system shows dendrite-free deposition/striping at the Al anode. The large voltage hysteresis can be effectively reduced by elevating the temperature. The scientific insights obtained in this work shed light on the electrochemical sulfur reaction in a tri-valent cation environment and will facilitate progress on the way to realize a rechargeable Al/S battery.

Acknowledgements

This work was supported as part of the Nanostructures for Electrical Energy Storage (NEES), an Energy Frontier Research Center funded by the U.S. Department of Energy, Office of Science, Basic Energy Sciences under Award number DESC0001160. We acknowledge the support of the Maryland NanoCenter and its AIM Lab. We thank Dr. Gil Cohn for his valuable comments.

Keywords: aluminum/sulfur batteries · electrochemistry · ionic liquids · solid-state reactions · sulfur

How to cite: *Angew. Chem. Int. Ed.* **2016**, *55*, 9898–9901
Angew. Chem. **2016**, *128*, 10052–10055

[1] L. Bai, B. E. Conway, *J. Electrochem. Soc.* **1990**, *137*, 3737–3747.
[2] T. Jiang, M. J. Chollier Brym, G. Dubé, A. Lasia, G. M. Brisard, *Surf. Coat. Technol.* **2006**, *201*, 1–9.
[3] H. Wang, S. Gu, Y. Bai, S. Chen, N. Zhu, C. Wu, F. Wu, *J. Mater. Chem. A* **2015**, DOI: 10.1039/C5TA06187C.
[4] P. R. Gifford, J. B. Palmisano, *J. Electrochem. Soc.* **1988**, *135*, 650–654.

[5] J. V. Rani, V. Kanakaiah, T. Dadmal, M. S. Rao, S. Bhavanarushi, *J. Electrochem. Soc.* **2013**, *160*, A1781 – A1784.
[6] T. Tsuda, I. Kokubo, M. Kawabata, M. Yamagata, M. Ishikawa, S. Kusumoto, a. Imanishi, S. Kuwabata, *J. Electrochem. Soc.* **2014**, *161*, A908 – A914.
[7] W. Wang, B. Jiang, W. Xiong, H. Sun, Z. Lin, L. Hu, J. Tu, J. Hou, H. Zhu, S. Jiao, *Sci. Rep.* **2013**, *3*, 3383.
[8] N. Jayaprakash, S. K. Das, L. A. Archer, *Chem. Commun.* **2011**, *47*, 12610.
[9] X. Ji, K. T. Lee, L. F. Nazar, *Nat. Mater.* **2009**, *8*, 500 – 506.
[10] R. Elazari, G. Salitra, A. Garsuch, A. Panchenko, D. Aurbach, *Adv. Mater.* **2011**, *23*, 5641 – 5644.
[11] Z. Zhao-Karger, X. Zhao, D. Wang, T. Diemant, R. J. Behm, M. Fichtner, *Adv. Energy Mater.* **2015**, *5*, 1401155.
[12] T. Gao, M. Noked, A. J. Pearse, E. Gillette, X. Fan, Y. Zhu, C. Luo, L. Suo, M. A. Schroeder, K. Xu, et al., *J. Am. Chem. Soc.* **2015**, *137*, 12388 – 12393.
[13] S. Xin, Y.-X. Yin, Y.-G. Guo, L.-J. Wan, *Adv. Mater.* **2014**, *26*, 1261 – 1265.
[14] S. Wenzel, H. Metelmann, C. Raiß, A. K. Dürr, J. Janek, P. Adelhelm, *J. Power Sources* **2013**, *243*, 758 – 765.
[15] G. Cohn, L. Ma, L. A. Archer, *J. Power Sources* **2015**, *283*, 416 – 422.
[16] A. C. Kozen, C.-F. Lin, A. J. Pearse, M. A. Schroeder, X. Han, L. Hu, S.-B. Lee, G. W. Rubloff, M. Noked, *ACS Nano* **2015**, *9*, 5884 – 5892.
[17] L. X. Yuan, J. K. Feng, X. P. Ai, Y. L. Cao, S. L. Chen, H. X. Yang, *Electrochem. Commun.* **2006**, *8*, 610 – 614.
[18] A. Swiderska-Mocek, E. Rudnicka, *J. Power Sources* **2015**, *273*, 162 – 167.
[19] M. Nagao, A. Hayashi, M. Tatsumisago, *Electrochim. Acta* **2011**, *56*, 6055 – 6059.
[20] S. Zhang, K. Ueno, K. Dokko, M. Watanabe, *Adv. Energy Mater.* **2015**, 1500117.
[21] G. Zhou, E. Paek, G. S. Hwang, A. Manthiram, *Nat. Commun.* **2015**, *6*, 7760.
[22] M. Helen, M. A. Reddy, T. Diemant, U. Golla-Schindler, R. J. Behm, U. Kaiser, M. Fichtner, *Sci. Rep.* **2015**, *5*, 12146.

Received: April 12, 2016
Published online: July 15, 2016

